Pergamon

Int. J. Heat Mass Transfer. Vol. 37, No. 16, pp. 2535–2546, 1994

0017–9310/94 $7.00+0.00

0017–9310(94)E0072–3

Cryogenic mixing with phase change in the simulation of LO_2/LH_2 explosion hazards: shallow mixing mode

E. Y. KWACK, T. S. LUCHIK and L. H. BACK

Jet Propulsion Laboratory, California Institute of Technology, Pasadena, CA 91109, U.S.A.

(*Received* 27 *January* 1993 *and in final form* 18 *February* 1994)

Abstract—Experiments simulating mixing of liquid oxygen (LO_2) and liquid hydrogen (LH_2) have been performed to investigate the potential threat to the RTGs (Radioisotope Thermoelectric Generators) from an explosion of these cryogens as a result of a launch vehicle accident. The influence of the bottom wall of a dewar (spilled mode) has been evaluated in this investigation by using a shallow dewar (38.7 cm I.D. and 30.5 cm tall). The jet size was 1.27 cm O.D. and the jet velocity was varied from 3.97 to 8.75 m s^{-1}. The jet dump duration times were 0.45 and 1.15 s. Gas temperatures and the boil-off of the hydrogen were measured using thermocouples and hot films. The general mixing behavior was observed with high speed video imaging.

1. INTRODUCTION

THE ACCIDENTAL mixing of liquid hydrogen (LH_2) and liquid oxygen (LO_2) has been the subject of study at the Jet Propulsion Laboratory (JPL) for several years [1]. This interest was spawned by the potential threat to a variety of spacecraft and their associated Radioisotope Thermoelectric Generators (RTGs) resulting from a launch vehicle accident where LH_2 and LO_2 are the propellants for the launch vehicle. The primary concern is that a detonable mixture of H_2 and O_2 will be formed in the vicinity of the RTG. However, the characteristics of such a mixture and resultant near-field detonation were neither well defined nor well understood. The existing data base [2] on H_2–O_2 detonations focused on the far-field characteristics.

From an explosion hazards perspective, it is during the initial mixing of the cryogenic propellants that a detonable mixture of hydrogen and oxygen is formed. The fluid dynamic mixing of LH_2 and LO_2 is an extremely difficult process to study because the resultant mixture is extremely volatile. However liquid nitrogen (LN_2) has proven to be an excellent simulant for LO_2 in earlier tests on LO_2–liquid helium (LHe) and LN_2–LHe mixtures [3, 4]. Removing the volatility of the mix does not simplify the fluid dynamics since the thermodynamic properties of the fuel and oxidizer (simulant) are so different. Each fluid is at or near its saturated vapor temperature, and these are different by more than 55 K (77 K for LN_2 and 20 K for LH_2, see more thermophysical properties in Table 1). Therefore, when the two fluids mix the fluid dynamics are extremely complex: LN_2 will tend to cool and finally freeze while LH_2 boils and superheats.

Two mixing scenarios are under investigation. The first one involves a jet of one fluid injected into a deep pool of the other. Earlier tests by Bishop *et al.* [5] showed that significant mixing occurred only when the oxidizer simulant was injected into a pool of liquid hydrogen. Later tests by Luchik *et al.* [6] involving a jet of LN_2 injected into a pool of LH_2 showed that jet mixing ceased some 150–200 ms after initial impingement of the jet on the free surface of the pool (for jet velocities up to 11 m s^{-1}). However, 50 to 150 ms after the jet was stopped, a second surge of jet fluid was observed. Maximum boiling of the H_2 occurred 200–300 ms after jet impingement and scaled with the jet nozzle diameter. This indicated that the rate of boiling was dependent on the surface area of the jet (i.e. the jet could be modeled as a column of fluid submerged in a pool of hydrogen). This was substantiated by a flash radiograph of the mixing zone which further indicated that the mass of fluid sheared from the jet was small. Visible imaging of the mixing zone showed

Table 1. Some properties of hydrogen, nitrogen and oxygen

	Hydrogen	Nitrogen	Oxygen
T_{BP} (K) (1 atm)	20.26	77.35	90.18
T_{FP} (K) (1 atm)	13.8	63.15	54.36
ρ_{BP_l} (kg m^{-3})	70	807	1141
ρ_{BP_g} (kg m^{-3})	1.3	4.6	4.5
h_{fg} (kJ kg^{-1})	454	199	213
h_{fs} (kJ kg^{-1})	—	25.1	13.8
$h_{\gamma-\beta}$ (kJ kg^{-1})	—	—	23.4
$T_{\gamma-\beta}$ (K)	—	—	43.8
$h_{\beta-\alpha}$ (kJ kg^{-1})	—	~8.4	2.9
$T_{\beta-\alpha}$ (K)	—	35.6	23.6
c_{p,BP_g} (kJ kg^{-1} K^{-1})	12.15	4.73	1.0
c_{p,BP_l} (kJ kg^{-1} K^{-1})	9.66	2.13	1.67
c_{p,FP_s} (kJ kg^{-1} K^{-1})	—	1.88	1.42

NOMENCLATURE

c_p	specific heat
h_{fg}	heat of vaporization
h_{fs}	heat of fusion
m	mass
Δm	integrated amount of mass
$\dot{m}$	mass flow rate
r	radial coordinate
t_d	dump duration
t_{in}	time when the jet impinges into host fluid
T	temperature
T_w	hot film temperature
u	axial velocity
z	vertical coordinate from bottom of dewar.

Greek symbol

ρ	density.

Subscripts

BP	boiling point
FP	freezing point
g	gas value
j	jet
l	liquid
min	minimum
s	solid.

that the frozen nitrogen particles first formed near the head of the jet 200–300 ms after jet impingement. From the motion of the particles they were determined to be platelet in shape and as large as several hundred square millimeters.

The work presented here represents the second of the mixing scenarios mentioned previously. In the present study, the presence of a wall at the base of the hydrogen pool (i.e. shallow pool) and its influence on the above parameters is investigated.

2. APPARATUS

This section gives a brief overview of the facility, instrumentation and procedures which are similar to the ones used in the deep mixing experiments. For more detailed description see Luchik *et al.* [3, 4, 7].

2.1. *Facility*

A schematic of the facility is shown in Fig. 1. The primary enclosure is mainly an exhaust duct for the liquid fuel that is boiled off during an experiment. This enclosure houses all plumbing for oxidizer simulant (LN_2) to the dump tank as well as for fuel liquid (LH_2) to the dewar. The stainless steel dump tank used in the experiments is 14.6 cm in diameter (dia.) and has a capacity of 10.4 liters. Flow out of the dump tank through a 1.27 cm dia. tube (Fig. 2) was controlled using a pneumatically operated cryogenic ball valve. Because of the nature of the experiments, knowledge of the valve timing was critical and hence, the valve was calibrated. Results of the calibrations showed that the valve, when operated at 100 psi, responded to the operator in 60 ms and went from the fully closed position to the fully open position in 40 ms. The detailed valve response is shown in a previous report [3]. The flow rate out of the dump tank or the injection velocity was controlled by regulating the pressure of the fluid inside the tank. The bottom of the primary enclosure is connected with the Pyrex glass experimental dewar through a metal bellow (15.24 cm dia., 30.4 cm long) and converging or cone section (15 cm long) (Fig. 2). The fuel LH_2 was transferred through a fill line (0.318 cm O.D.). The dewar has a diameter of 38.7 cm and is 30.5 cm in height. The dewar was not specially designed for cold cryogen application, having no vacuum jacket but is commercially available. Our prior experience with a large vacuum jacketed dewar was that it fractured at the top lip when subjected to cryogenic fluids. Since the dewar has no vacuum jacket, some of the N_2 purge gas in the secondary enclosure solidified on the outer surface to obstruct the view when it was filled with LH_2. Located at the top of the primary enclosure, was a 10.2 cm diameter exhaust stack. The exhaust gas then flowed into a dilution duct where the exhaust fuel was diluted below its flammability limit and was exhausted to the atmosphere.

As shown in Fig. 1, the primary enclosure was located inside the secondary enclosure which is a small room 3.66 m on a side. The secondary enclosure was purged free of oxygen prior to each experiment and the oxygen level was monitored throughout the experiments using a Teledyne Analytical Systems Model 8000 gas detection system. Purging served two purposes. First, removing all of the air (oxygen) excludes the possibility of an accidental explosion during an experiment. Second, removing all of the air (oxygen) from the experiment and replacing it with nitrogen greatly enhanced the visual observation of the experiment, since no water vapor was available in the environment to condense and freeze on the outside of the experimental dewar. This purging of the secondary enclosure and diluting of the fuel exhaust was accomplished using an inert gas purge system.

2.2. *Instrumentation*

Chromel–constantan thermocouples (type E) were chosen for these experiments based on arguments presented by Barron [8] and ASTM [9]. Because the experiments performed are transient in nature, the temporal response of the instrumentation is quite

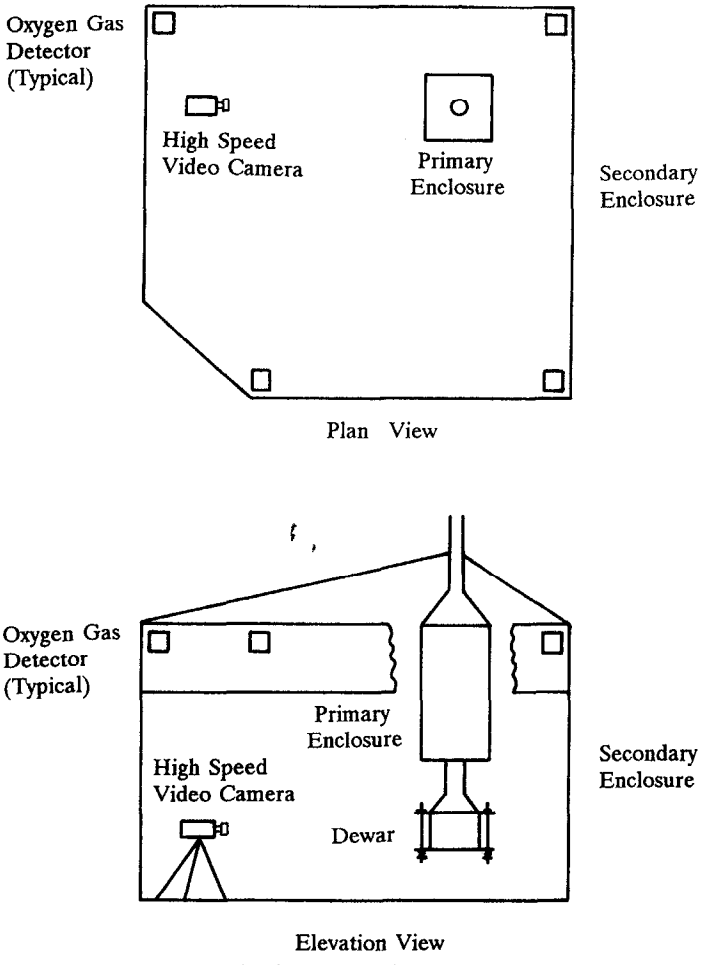

FIG. 1. Schematic of primary and secondary enclosures.

important. The size of the thermocouples chosen for the experiments was 76 μm which had a response time of about 8 ms (90%). This size was a good compromise between speed and robustness (the experiments were fairly violent and smaller thermocouples did not survive the environment with regularity). Six thermocouples were installed at five different vertical locations, being 5.08 cm off from the center of the dewar (Fig. 2). The lowest one was located 15.2 cm above the bottom of the dewar. The spacing between thermocouples was 7.62 cm. Two thermocouples were used at the inlet of the metal-bellow. Radial and circumferential temperature profiles were measured at the top of the dewar ($z = 30.5$ cm). The radial locations were $r = 5.08$, 8.89, 12.7 and 16.5 cm. The circumferential temperature profile was measured at $r = 12.7$ cm.

Cryodiodes were used in locations where sub-40 K temperatures were expected. Four cryodiodes were located along the side wall of the dewar (Fig. 2). The lowest one was 5.08 cm from the bottom of the dewar and the spacing between the cryodiodes was 5.08 cm. Two cryodiodes were installed in the dump tank to monitor the level of LN_2. The sensitivity of a cryodiode is excellent at low temperatures. However, the cryodiode does have two major disadvantages. The diodes have response times which varied with the ΔT due to the large thermal capacitance of the can housing the diode. Times as great as 2 s were measured for a ΔT of 200 K. Although the diodes were quite robust themselves, the wiring to the diode was delicate and often broke during experimentation.

Pressures in the dewar, primary enclosure and in the dump tank were measured using Validyne pressure transducers. The transducers are fairly standard strain gage type transducers. Temperature effects at the transducer were minimized by using a length of Tygon tube from the point of measurement to the transducer, which was maintained nominally at 300 K.

Hot film anemometers were used to measure velocities of the fuel boil-off gas at the inlet of the metal bellow above the dewar (Fig. 2). The hot-films were calibrated over a range of temperatures and velocities. Details of the hot film calibrations are given by Kwack *et al.* [10]. The low temperatures tended to destroy hot films after repeated cycling.

A Spin Physics model SP-2000 high speed motion analyzer was used to obtain video recordings of each

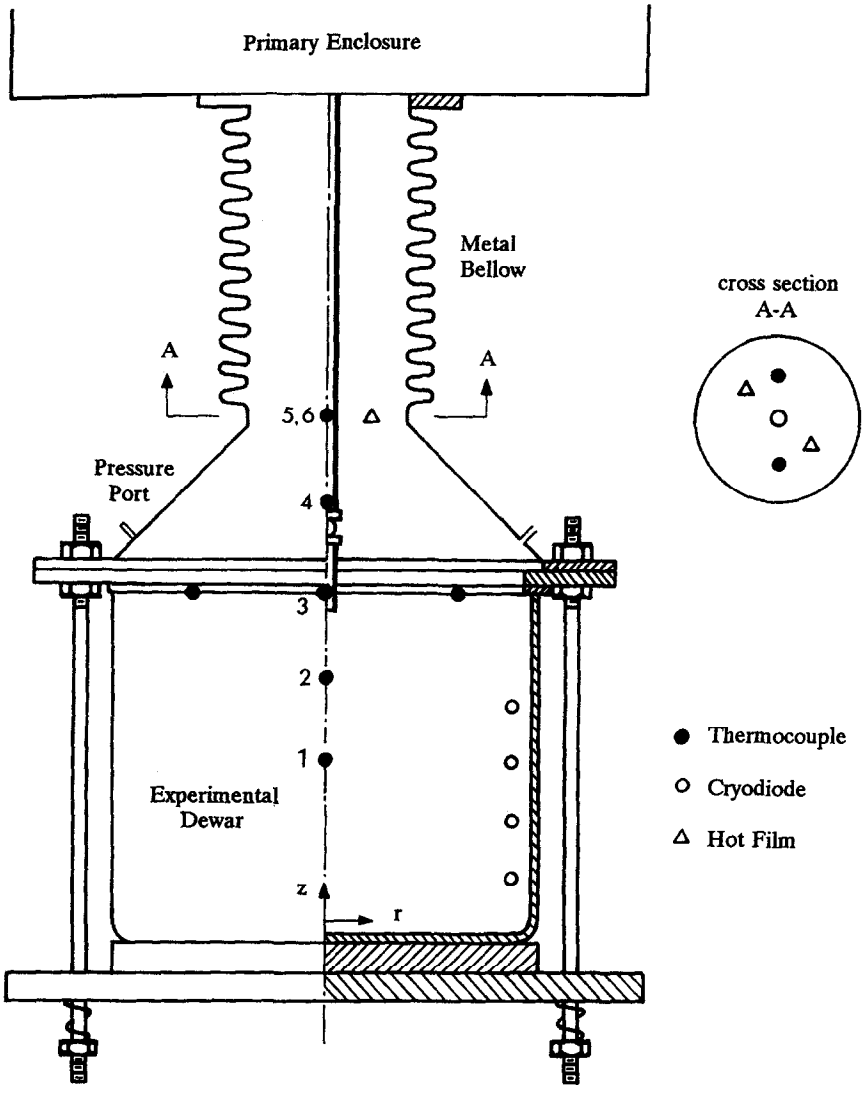

FIG. 2. Schematic of experimental apparatus.

experiment. For these experiments, recordings were obtained in excess of 1000 fps. Typically, the vertical field of view was 45 cm with a minimum spatial resolution of 2.2 mm × 2.2 mm. The experiment was back lighted with two quartz halogen lights.

Data acquisition during tests is accomplished using the high speed A/D boards. The host computer is an IBM PC compatible. The main function of the compatible during data acquisition is as a memory device for the high speed A/D boards. Data sampling occurs over 26 channels at a rate of 100 scans s^{-1}. The hot wire/film, cryodiode and pressure transducer data are fed directly into the A/D boards while the thermocouple information must be passed through an intermediate amplifier. The A/D board signals the host computer at appropriate times to trigger the dump tank operator valve. The host achieves the triggering process though the use of a parallel I/O board and relay board. The host computer also controls the Spin Physics motion analyzer through an RS-232 port.

3. RESULTS AND DISCUSSION

The mixing behavior of two cryogens in a shallow dewar was inferred from the observation for two dump duration times (t_d = 0.45 and 1.15 s) with various jet velocities from 3.97 to 8.75 m s^{-1} (see Table 2). Figure 3 shows the general mixing dynamics for this experimental configuration, the shallow mixing mode. In general the warmer jet fluid (LN_2) cools down as it penetrates the colder pool fluid (LH_2) and eventually freezes, while the pool fluid boils at the mixing zone interface. The frontal edge of the jet becomes flattened due to the high vapor pressure build-up by rapid boiling of the host fluid there and forms many droplets at the outer edge due to shearing

Table 2. Summary of experimental tests

t_d (s)	u_j (m s^{-1})	t_{in} (s)	m_{N_2} (g)	Δm_{H_2}† (g)
0.45	3.97	0.22	182.7	104.4
0.45	7.16	0.15	329.4	123.5
0.45	7.70	0.14	346.5	143.8
0.45	7.99	0.14	367.6	164.3
0.45	8.63	0.12	397.1	191.4
1.15	3.97	0.22	466.8	212.1
1.15	6.98	0.15	820.7	318.6
1.15	7.16	0.15	841.9	314.5
1.15	7.50	0.14	881.9	310.5
1.15	7.77	0.14	913.6	350.5
1.15	8.75	0.13	1029	387.0

†Integrated values from $t = 1$ to $t = 9$ s.

forces. During this time period, there may be two different mechanisms to produce solid jet particles: (i) droplets of the jet liquid formed by the Helmholtz instability become solid and (ii) the surface of the jet becomes solid by heat transfer to the host fluid and is sheared off, becoming platelet shaped solid particles. Before the jet reaches the bottom of the dewar the general behavior of mixing is the same as that in the case of the deep mixing mode, for which the detailed description can be found in the earlier reports [4, 6].

After the jet reaches the bottom of the dewar, the jet spreads radially becoming thin cylindrical plate-like in shape. Some of the jet fluid may splash at the stagnation point on the bottom wall. The front portion of the jet fluid slows down as it penetrates radially further along the bottom of the dewar, since the frontal area increases proportional to the radius. The evaporated gas of the host fluid (GH_2) moves toward the center of the dewar and moves vertically upwards through the already formed mixing zone. More solid particles of the jet fluid are believed to be formed during this stage because more jet fluid contacts the cold host fluid and the bottom surface of the dewar. The surface of the top side of the jet fluid spreading radially may become solid by heat transfer to the host fluid, and at the bottom side of the jet, fluid is chilled by the cold bottom surface of the dewar which is initially very close to the boiling temperature of the host fluid. When the jet velocity is high, some of the vaporized gas rises vertically through the pool fluid, not through the already formed mixing zone because of the rapid formation of GH_2. The jet eventually reaches the side wall of the dewar, if the dump duration time is long enough, and can move upwards along the side wall.

In addition, a quasi-one-dimensional, parametric model has been developed to describe the detailed interation of a warmer cryogen jet (LN_2, LO_2) injected into a static pool of colder cryogen (LHe, LH_2) by Harstad [11]. The detailed heat transfer, and vapor and particle production are estimated.

Figure 4(a) shows instantaneous temperatures of H_2 gas at several different vertical locations measured 5.08 cm away from the center of the jet (or the dewar) before, during and after the dump. The corresponding instantaneous evaporation rate of H_2 gas is presented in Fig. 4(b). The jet velocity was 3.97 m s^{-1} and the dump duration was 0.45 s. The initial level of LH_2 was 14 cm above the bottom of the dewar ($z = 14$ cm). LH_2 boils off even without mixing with LN_2 due to heat transfer from the surroundings. The normal boil off rate is about 4–5 g s^{-1} (Fig. 4b) before the LN_2 spill. The gas temperatures near the surface of LH_2 ($z = 15$ cm) were very close to the boiling temperature of 20K for LH_2 during the entire test. Table 1 lists some physical properties of hydrogen, nitrogen and oxygen. More information on cryogenic fluid properties can be found in McCarty *et al.* [12], Barron [8], Sychev *et al.*, [13, 14] and Scott [15]. Before the LN_2 spill the vaporized hydrogen was warmed up during rising by heat transfer from the surroundings, and reached about 105 K at the outlet of the test section ($z = 45.7$ cm) where the vaporized H_2 gas exited

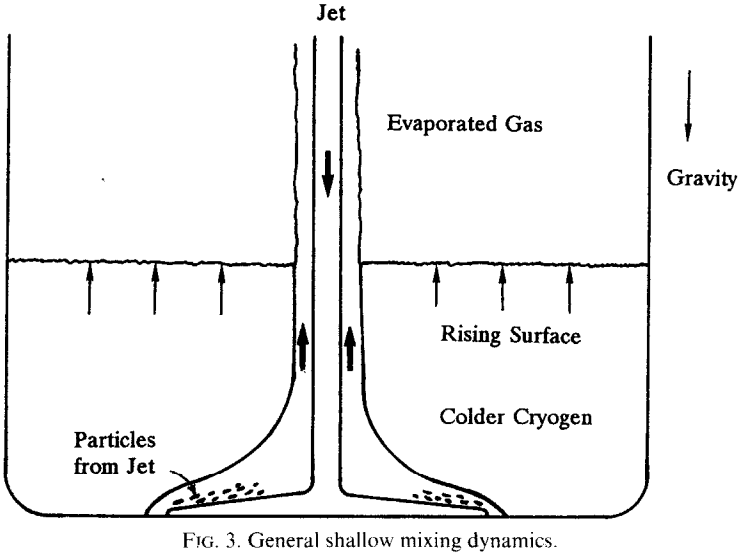

FIG. 3. General shallow mixing dynamics.

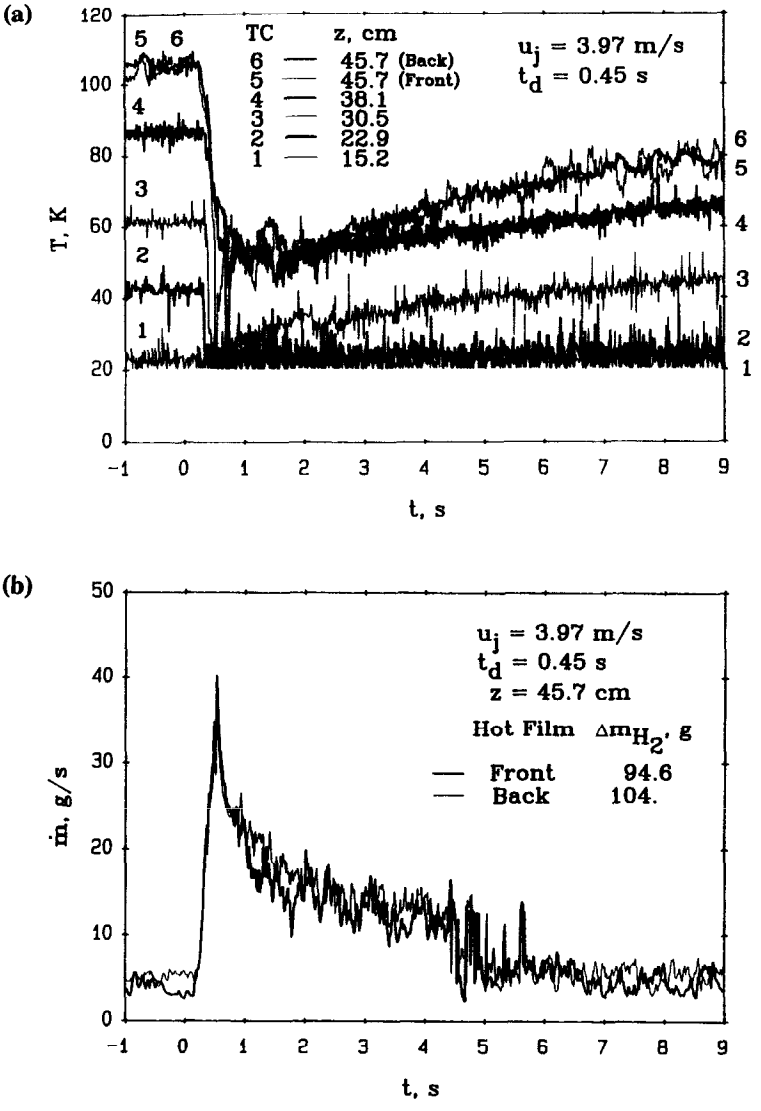

FIG. 4. (a) Instantaneous vertical temperature profiles in the test section and (b) instantaneous evaporation rate of H_2 gas for the jet of $u_j = 3.97$ m s^{-1} and $t_d = 0.45$ s.

through the metal bellow to the primary enclosure. There the gas temperature was measured with two thermocouples at two different circumferential locations (Fig. 2) and both readings agreed well with each other (lines 5 and 6 in Fig. 4a). In some tests, there were some differences between these gas temperatures. Two hot films were used to measure the evaporation rate of H_2 gas at the same vertical location ($z = 45.7$ cm) and these measurements are close to each other (Fig. 4b). The gas temperatures were quite steady before the LN_2 spill and mixing, and show quite a significant vertical temperature gradient of about 2.8 K cm^{-1}.

Jet impingement occurred about 0.23 s after the dump valve was energized ($t = 0$) and caused the vaporization of much more hydrogen gas. As the jet penetrated further the rate of evaporation increased (Fig. 4b). As the rate of evaporation increased, the gas exited the test section without exchanging much heat with the surroundings because the gas residence time in the test section decreased. Therefore, the gas temperatures in the test section decreased as shown in Fig. 4(a). Since this newly formed GH_2 by mixing pushes the preformed GH_2 upward by normal boiling before mixing, the gas temperatures decrease somewhat gradually before newly formed cold H_2 gas passes. For example, the gas temperature near the exit of the test section ($z = 45.7$ cm) starts decreasing at $t = 0.25$ s which is about 20 ms after jet impingement.

Since the rate of evaporization increases very rapidly during initial mixing, the edge of newly formed GH_2 by mixing was clearly observed. When the vaporized cold H_2 gas formed by mixing passes the thermocouple, the reading suddenly decreases so that this is a good indication of the rising motion (the outer edge) of the vaporized H_2 gas by mixing. The cold vaporized H_2 gas passes TC2 ($z = 22.9$ cm) and TC3 ($z = 30.5$ cm) at $t = 0.31$ and 0.37 s, respectively. The

average rising velocity of the H_2 gas between these two locations is about 1.3 m s^{-1} which agrees well with visual observation. The gas temperature at the TC5 ($z = 45.7$ cm) is seen to decrease faster at $t = 0.42$ s which may indicate passing of the cold GH_2 formed by mixing.

As the jet penetrates the LH_2 further, the mixing surface area increases. The area also increases more because the surface of LH_2 rises. The mixing area increases much faster after the jet reaches the bottom of the dewar and spreads radially. When the mixing area increases, the heat transfer increases which results in producing more GH_2. The rate of heat transfer from LN_2 to LH_2 and the walls becomes equal to the incoming rate of energy into the mixing zone by the jet. At the same time, the evaporation rate reaches a maximum value and persists for awhile if the dump time is long enough which will be shown later for longer dumps. Then the heat transfer rate decreases when the dump valve starts closing. In other words, the evaporation rate of H_2 gas starts decreasing even though the jet fluid still is supplied into the mixing zone. The experimental results supports this idea. The maximum evaporation rate occurs at $t = 0.52$ s (Fig. 4b) which is very close to the time when the dump valve starts closing. This is earlier than the time when the last portion of the jet fluid passed the initial LH_2 level ($t = 0.68$ s). If it is assumed that the level of LH_2 rose over the exit of the nozzle, t would be 0.65 s. After it reaches a maximum value, the evaporation rate decreases sharply and then gradually decreases, as solid nitrogen particles descend and the vigorous motion of boiling liquid hydrogen continues to settle down. In the meantime, the gas temperatures at the different vertical locations decrease rather sharply, reach minimum values, remain at those values for awhile and increase gradually. Of note is that the readings of TC4 and TC6 reach very low values close to the LH_2 boiling temperature momentarily (for ~ 50 ms). This could be caused by LH_2 drops or small SN_2 particles carried by GH_2 which would then be vaporized or dislodged. Big SN_2 particles may not cool down to the LH_2 boiling temperature. The gas temperatures were measured at four different radial locations ($r = 5.08$, 8.89, 12.7 and 16.5 cm at $z = 30.5$ cm) and did not vary much. The gas temperatures at the four circumferential locations (90° apart) were also measured at $z = 30.5$ cm and $r = 12.7$ cm and they showed some differences during the initial couple of seconds, but they then became the same.

The jet velocity was varied from 3.97 to 8.63 m s^{-1} for the same dump duration, $t_1 = 0.45$ s to evaluate the jet momentum effects on the mixing. As the jet velocity increases jet impingement occurs earlier which varies from 0.22 s for $u_j = 3.97$ m s^{-1} down to 0.12 s for $u_j = 8.63$ m s^{-1} (see Table 2). When the jet velocity is higher than 7.16 m s^{-1}, the gas temperature at the exit of the test section $z = 45.7$ cm reaches the normal boiling temperature of LH_2 and remains at that value longer as the jet velocity increases (Fig. 5a). A sudden temperature change occurs at $t \simeq 4$ s for $u_j = 8.63$ m s^{-1} which may be due to solid nitrogen particles or drops of liquid hydrogen settling on the thermocouple and eventually being dislodged or evaporated by the gas.

When the jet velocity is higher than 7.16 m s^{-1}, the evaporation of GH_2 shows a very sharp spike at the beginning of mixing which could be due to initial splashing of LH_2 when the jet impinges into LH_2 (Fig. 5b). After the initial spike, the evaporation rate increases again but gradually, and reaches a maximum value which becomes larger as the jet velocity increases. Several sharp spikes were observed for $u_j = 8.63$ m s^{-1} after the evaporation rate was maximum. This could be due to the LH_2 or SN_2 which were carried by H_2 gas. If they were small droplets or particles, they could be vaporized very fast because the wall temperature of the hot film is relatively high ($T_w = 191.7$ K). If u_j is higher than 7.16 m s^{-1}, the rates of decrease in $\dot{m}$ are very steep initially and somewhat less at $t \simeq 0.6$ s which is close to the end of dump. If no more jet fluid is supplied, the opening of the mixing zone in the LH_2 pool will be closed-up. Then, since it will take more time for GH_2 to escape from LH_2, the rate of evaporation would slow down.

The amount of solid nitrogen produced during mixing is proportional to the amount of the liquid nitrogen dumped. Some of the SN_2 particles were probably carried upwards by GH_2 and then descended later. Since these solid nitrogen particles were warmed-up by the surroundings, they vaporized H_2 gas when they later descended into the LH_2 pool. In addition, the high velocity jet introduced more disturbances in the LH_2 pool. Therefore, the evaporation rate remains higher for awhile when the jet velocity was higher (Fig. 5b). Then the evaporation rates at various jet velocities eventually became the same as time passes. The evaporation rate for $u_j = 7.16$ m s^{-1} becomes the same as that for $u_j = 3.97$ m s^{-1} at $t = 1$ s, whereas at higher jet velocities of $u_j = 7.99$ and 8.63 m s^{-1}, the times were progressively larger being $t = 1.4$ and 1.6 s, respectively (Fig. 5b).

Similar tests were performed for a longer dump time, $t_d = 1.15$ s. The gas temperatures at the exit of the test section $z = 45.7$ cm are shown for various jet velocities from 3.97 to 8.75 m s^{-1} in Fig. 6(a). Compared to the shorter dump ($t_d = 0.45$ s, in Fig. 5a), the gas temperature generally remains at the hydrogen boiling temperature for a longer time since more hydrogen gas was produced during the mixing for the longer dump. Corresponding instantaneous evaporation rates $\dot{m}$ are shown in Fig. 6(b) for only three jet velocities to avoid too much overlap. For the longer dumps, the values of the maximum $\dot{m}$ are larger than those for short dumps if the jet velocities are the same. There are more spikes especially at the highest jet velocity, $u_j = 8.75$ which probably means that more LH_2 drops or SN_2 particles were carried upward in the H_2 gas boil-off.

The values of the evaporation rate $\dot{m}$ were inte-

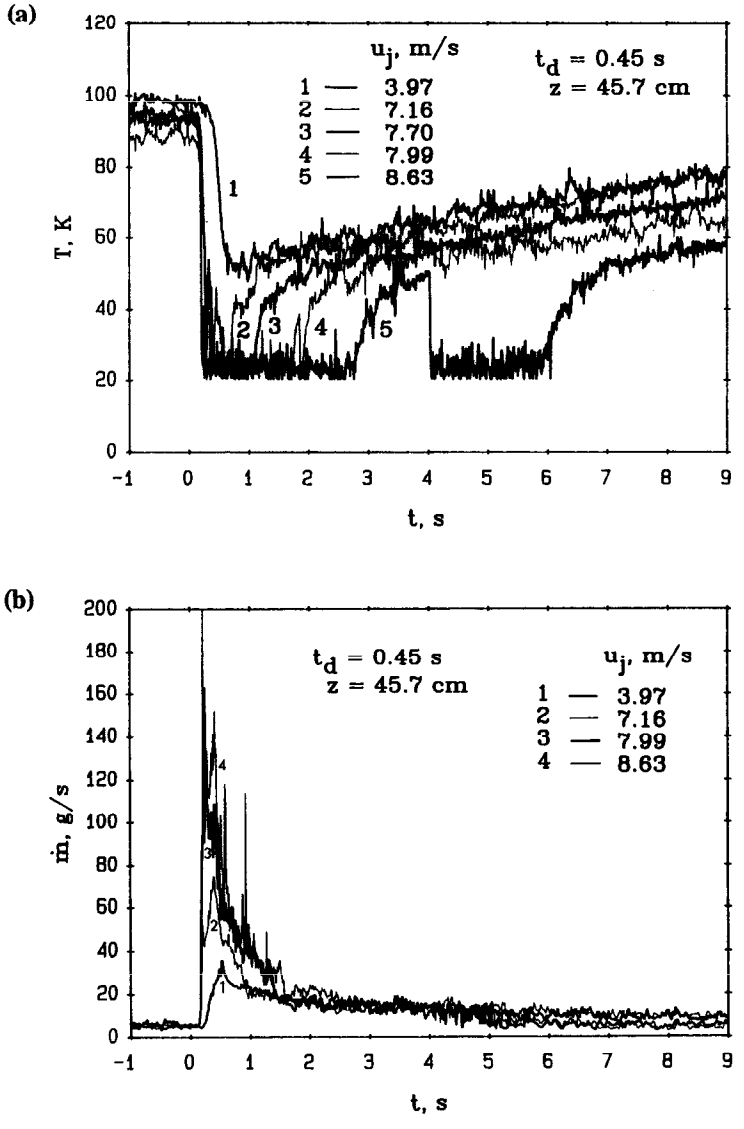

FIG. 5. (a) Instantaneous temperature at the exit of the test section and (b) instantaneous evaporation rate of H_2 gas for various jet velocities from 3.97 to 8.63 m s^{-1} with $t_d = 0.45$ s.

grated with time, Δm_{H_2} and the results are shown in Fig. 7(a) for the longer dump tests. The amount of hydrogen boil-off increases rapidly during the dump and then gradually increases at the later times. As the jet velocity or the amount of liquid nitrogen dumped increases, the total amount of hydrogen boil-off increases from 204.5 g for $u_j = 3.97$ m s^{-1} to 375.2 g for $u_j = 8.75$ m s^{-1} for 9 s after the dump valve was energized. The rate of increase in H_2 gas production strongly depends on the jet velocity during the first 1.5 s, being higher for the higher jet velocity. Therefore, most of the major mixing must occur during the dump. After that, hydrogen boils off mostly because of heat transfer from the surroundings instead of the mixing. This observation is also consistent with the results from the deep mixing mode tests. The major mixing occurs during an initial period less than twice the dump time for the deep mixing mode. Seemingly, the major mixing for the shallow mixing mode should last less time than that for the deep mixing since the jet spreads more in the shallow mixing mode and exposes more surface area for boiling LH_2 sooner.

The values of LH_2 boil-off for the longer dump tests, Δm_{H_2}, were divided by the total amounts of the jet fluid dumped and are shown in Fig. 7(b). In general, similar behavior was observed for the ratio of the hydrogen boil off to the total liquid nitrogen added as was seen in Fig. 7(a). The ratio increases rapidly during the mixing and then gradually increases. However, it is seen that the ratio does not strongly depend on the jet velocity. If it is assumed that the temperature of the mixing zone is the hydrogen boiling point which implies that the hydrogen boils off and leaves the mixing zone at its boiling point and that the nitrogen cools down to the hydrogen boiling point, the ratio $\Delta m_{H_2}/m_{N_2}$ is 0.27. The detailed

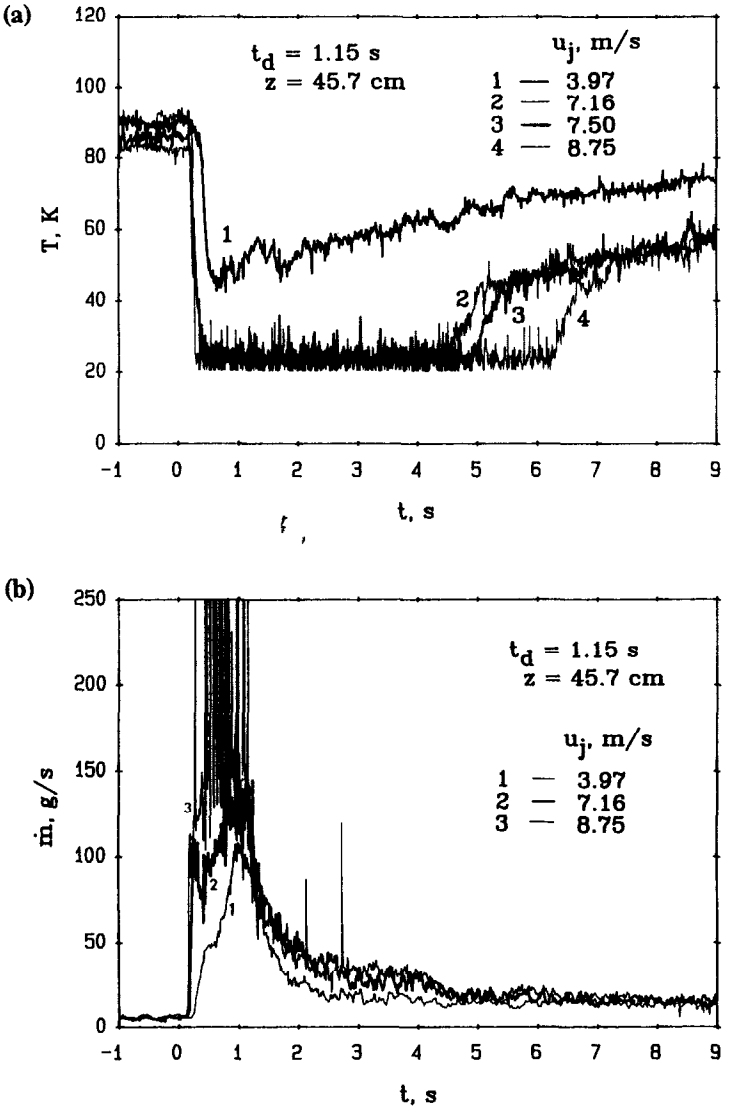

FIG. 6. (a) Instantaneous temperature at the exit of the test section and (b) instantaneous evaporation rate of H_2 gas for various jet velocities from 3.97 to 8.75 m s^{-1} with t_d = 1.15 s.

calculation obtained from a global energy balance was reported in the previous paper [6]. If the temperature of the mixing zone increases, this ratio decreases. For example, the values of ratio are 0.255, 0.226 and 0.200 when the temperatures of the mixing zone are 22, 26 and 30 K, respectively.

Figure 7(b) indicates that the experimental ratios $\Delta m_{H_2}/m_{N_2}$ are about 0.2 at t = 2 s when most of the major mixing has occurred. There are several possible reasons why the ratio may be smaller than 0.27 at t = 2 s. They are (1) the temperature of the mixing zone was higher than the hydrogen boiling point, (2) some of the solid nitrogen particles were carried away before they were cooled down to the mixing zone temperature, (3) still some amount of LN_2 or SN_2 remained in the LH_2 and (4) there was heat loss from the LN_2 jet fluid to the bottom and the side wall of the dewar during mixing.

The possible contribution of each of these items were estimated. For item (1), the ratio is 0.2 if the temperature of the mixing zone is 30 K. However, the experimental results show very little increase of gas temperature above the boiling point (2 or 3 K at most) which could be within the accuracy of the thermocouple. If the mixing zone temperature is 22 K, the ratio is 0.255 which is still much higher than 0.2. For item (2), some of the solid nitrogen particles can be carried away before they have been cooled down to the mixing zone temperature, if their sizes are large enough to have a high thermal mass. Visual observation shows that some of the solid nitrogen particles are as large as 4–5 mm on the long side. Since the residence time of a particle in the mixing zone is shorter than 400 ms which was estimated based on the maximum linear length of the mixing zone of 40 cm and a gas velocity of 1 m s^{-1}, particles larger than 1 mm would not be cooled down to the mixing zone temperature. Some experimental results support this

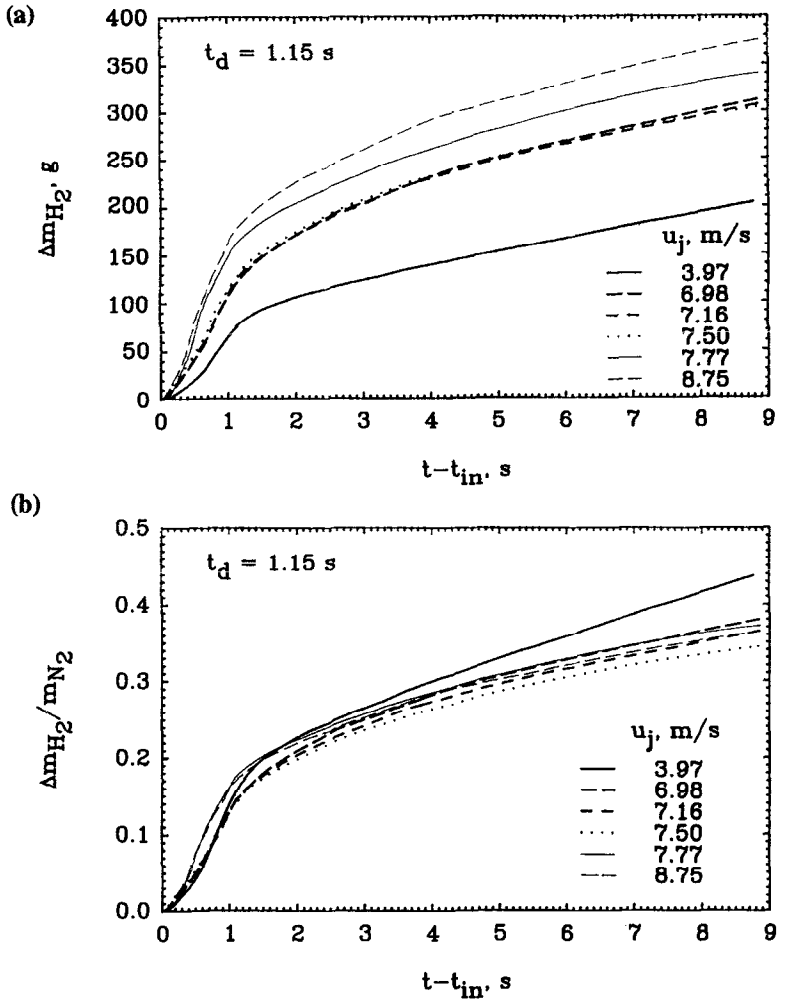

FIG. 7. (a) Integrated amounts of the evaporated H_2 gas vs $t-t_{in}$ and (b) mass ratios of the integrated amounts of the evaporated H_2 gas to the dumped LN_2 vs $t-t_{in}$ for various jet velocities from 3.95 to 8.75 m s^{-1} with t_d = 1.15 s.

idea. Figure 8 shows the reading of thermocouples at z = 30.5 cm and 45.7 cm for u_j = 3.97 m s^{-1} and t_d = 1.15 s. After the jet impinged into LH_2, both readings reached values near the hydrogen boiling point. Then the reading of the thermocouple at z = 30.5 cm suddenly jumped up to about 60 K during the jet dump time and then gradually decreased, while the output of the thermocouple at z = 45.7 cm stayed near the hydrogen boiling point during the entire dump and then increased. Therefore, solid nitrogen particles whose temperature was somewhat higher, about 60 K, were likely carried by GH_2, stuck on the thermocouple and were then cooled down by cold GH_2. However, since large particles tend to remain in the mixing zone, only a small fraction of the total dumped fluid can be carried away from the mixing region. Even though it is assumed that 5% of the total mass of LN_2 was carried away as solid particles at T = 60 K, the ratio is still 0.263 (relatively small change from 0.27) since the specific heat of solid nitrogen is rather small.

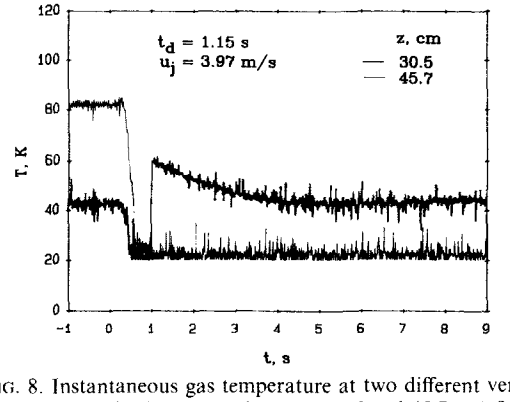

FIG. 8. Instantaneous gas temperature at two different vertical locations in the test section (z = 30.5 and 45.7 cm) for u_j = 3.97 m s^{-1} with t_d = 1.15 s.

For item (3), after the dump valve was closed all the jet fluid kept spreading over the bottom wall of the dewar and the thickness of the layer became thinner. Most of the jet fluid was likely involved in the

heat transfer with the host fluid and with the bottom wall of the dewar. Therefore, not much jet fluid was left at $t = 2$ s for heat exchange, even though some of the SN_2 may have been at a higher temperature than the hydrogen boiling point. However, the specific heat of SN_2 is small, so that these contributions were very small. If it was assumed that 5% of the total LN_2 was left over the experimentally measured ratio $\Delta m_{H_2}/m_{N_2}$ would have been 0.21 instead of 0.2, which is a small change.

For item (4), the heat loss to the bottom and the side wall of the dewar was not easy to estimate since the jet penetration velocity could not be measured. If the other possibilities (1), (2) and (3) were neglected, about 25% of the LN_2 was cooled down to the hydrogen boiling point by heat loss to the bottom or the side wall of the dewar. If the previous assumptions are valid, the ratio was estimated to be 0.248. Then, the heat loss to the bottom and the side wall of the dewar was still significant, being about 15%. Therefore, the influence of the bottom and the side wall of the dewar is believed to be one of the most important factors that controls the mixing process.

A more closer look at the ratios $\Delta m_{H_2}/\Delta m_{N_2}$ during the dump could provide some evidence to previous discussion. During the dump, $(t - t_{in}) < t_d$, the values in Fig. 7(b) should be modified because the amount of the dumped nitrogen increases during the dump. The integrated amount of hydrogen boil-off, Δm_{H_2} was divided by the integrated amount of LN_2 during the same time, Δm_{N_2} for $u_j = 3.97$ m s^{-1} and 8.75 m s^{-1} and the ratios are shown in Fig. 9. The dump rate of LN_2 could vary during the valve opening and closing. However, the detailed dump rates were not known so that the average dump rate was used. After the dump $(t - t_{in}) > t_d$, the results are the same as those in Fig. 7(b). For $u_j = 8.75$ m s^{-1}, the ratio increases and reaches a plateau (= 0.18) at $t - t_{in} \simeq 0.5$ s. The reason could be as follows. When the jet reaches the bottom wall, it warms the bottom wall which is close to the boiling temperature of LH_2 initially. The bottom wall temperature gradually increases and reaches the asymptotic value at 0.5 s after the jet impinged into LH_2. For the lower velocity jet $u_j = 3.97$ m s^{-1}, it takes a longer time (about 1 s) to reach a plateau, and the plateau is a little lower, being 0.16. If the ratios are 0.18 and 0.16, the possible maximum heat loss to the walls are 33 and 41%, respectively. When the dump time was shorter ($t_d = 0.45$ s), similar trends were observed as seen in Fig. 9. However, the ratios were lower than those for longer dump times.

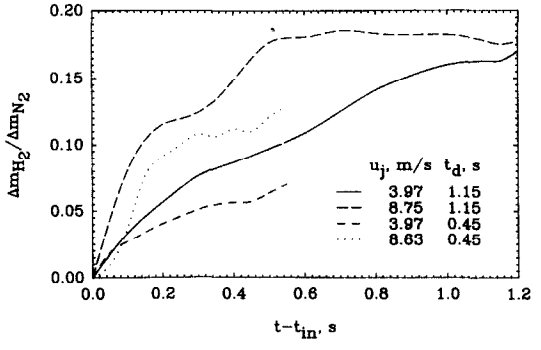

FIG. 9. Mass ratios of the integrated amounts of the evaporated H_2 gas to the dumped LN_2 during the dump.

The data shown in Fig. 9 do indicate that for early times considerably less hydrogen boil-off occurred than would be the case for global adiabatic mixing. Presumably in the shallow mixing mode, an appreciable fraction of the thermal energy of the LN_2 spilled into the LH_2 pool is lost by heat transfer to the relatively cold bottom and side wall of the container as the jet fluid spreads over the surface.

4. SUMMARY

JPL has conducted cryogenic mxing experiments to investigate the potential threat to the RTGs (Radioisotope Thermoelectric Generators) from an explosion of cryogens LO_2/LH_2 as a result of a launch vehicle accident. Since LN_2 has been found to be an excellent simulant for LO_2 in all aspects except the size of solid particles formed, LN_2 has been used for the non-reactive mixing experiments at JPL. The influence of the bottom wall of a dewar (spilled mode) has been evaluated in this investigation by using a shallow dewar (38.7 cm I.D. and 30.5 cm tall). The jet size was 1.27 cm O.D. and the jet velocity was varied from 3.97 to 8.75 m s^{-1}. The jet dump duration times were 0.45 and 1.15 s. Gas temperatures and the boil-off of hydrogen were measured using thermocouples and hot films. The general mixing behavior was observed with high speed video imaging.

The temperature of the hydrogen gas leaving the mixing zone was very close to the boiling point. The boil-off rate of hydrogen increased as the jet velocity and/or the dump duration increased. Liquid hydrogen drops and solid nitrogen particles were carried by the vaporized hydrogen gas during mixing. After the jet reached the bottom of the dewar, the jet spread over the bottom wall of the dewar which may enhance the mixing by increasing the mixing interface. However, the contact area of LN_2 and the bottom surface also increased at the same time which may increase the heat loss to the bottom wall. The mass ratio of the hydrogen boil-off to the nitrogen added during the mixing varied with the jet velocity and the dump duration. In general, the mass ratio increased during the initial jet penetration and reached an asymptotic value at the end of the dump for given conditions. These values were found to be lower than 0.27 which was estimated by assuming that the mixing zone temperature is the same as the hydrogen boiling temperature so that the temperature of hydrogen gas leaving the mixing zone and solidified nitrogen in the mixing zone are the same as the hydrogen boiling point. The mass ratio was as low as 0.16 for a dump duration of 1.15 s which implies that about 41% of the jet fluid energy was transferred to the bottom and

side walls of the dewar which was close to the hydrogen boiling temperature. The percentage amount of heat loss to the dewar walls could be much higher for short dumps.

Since the jet spreading on the bottom wall for shallow mixing enhances the mixing as well as the heat loss to the bottom wall as explained in the text, the following differences can be expected when the results are compared to those for the deep mixing mode with the same initial conditions. First, the peak boil-off rates for the shallow mixing mode can be higher than those for the deep mixing mode. Secondly, the mass ratios, $\Delta m_{H_2}/\Delta m_{N_2}$ during the mixing can be lower for the shallow mixing mode than those for the deep mixing mode.

Acknowledgements—The work described in this paper was carried out in the Applied Technologies Section of the Jet Propulsion Laboratory, California Institute of Technology, under Contract with the National Aeronautics and Space Administration. The encouragement of R. E. Wilcox, Launch Approval Engineering for the JPL Flight Project Office, and L. Reinhart and P. Jaffe, of the Accident Hazards Evaluation Program, is gratefully acknowledged. The assistance of W. Bixler, S. Kikkert and K. Harstad throughout the work is gratefully acknowledged.

REFERENCES

1. P. F. Massier, J. W. Marshall and R. M. Clayton, Liquid oxygen/liquid hydrogen explosion hazards program plan, JPL D-5113, Jet Propulsion Laboratory, Pasadena, California (1988).
2. A. B. Willoughby, C. Wilton and J. Mansfield, Liquid propellant explosive hazards, AFRPL TR-68-92, URS Research Company (1968).
3. T. S. Luchik, K. M. Aaron., E. Y. Kwack, P. Shakkottai, R. M. Clayton and L. H. Back, Cryogenic mixing processes in the simulation of LO_2/LH_2 explosion hazards: results with LN_2/LHe and LO_2/LHe, JPL D-6987, Jet Propulsion Laboratory, Pasadena, California (1990).
4. T. S. Luchik, K. M. Aaron, E. Y. Kwack, P. Shakkottai and L. H. Back, Cryogenic mixing with phase change in the simulation of LO_2/LH_2 explosion hazards, *Proceedings of the Ninth International Heat Transfer Conference*, Vol. 1, pp. 365–382. Hemisphere, New York (1990).
5. C. V. Bishop, F. J. Benz and L. J. Ullian, Mixing of cryogenic fluids and predicted detonation properties for multi-phase liquid oxygen and liquid hydrogen, Presented at the 1986 JANNAF Propulsion Meeting (1986).
6. T. S. Luchik, E. Y. Kwack, K. M. Aaron, P. Shakkottai and L. H. Back, Multi-phase mixing of liquid cryogens in the simulation of explosion hazards, *Int. J. Heat Mass Transfer* **317,** Suppl. 1, 123–132 (1994).
7. T. S. Luchik, K. M. Aaron, G. Fabris, R. M. Clayton and L. H. Back, Cryogenic mixing processes in the simulation of LO_2/LH_2 explosion hazards: experimental facility and initial results with LN_2/LHe, JPL D-6394, Jet Propulsion Laboratory, Pasadena, California (1989).
8. R. F. Barron, *Cryogenic Systems* (Monographs on Cryogenics), pp. 13–58. Oxford University Press, New York (1985).
9. *Manual on the Use of Thermocouples in Temperature Measurements*, ASTM special publication 470A, American Society for Testing and Materials, Philadelphia (1974).
10. E. Y. Kwack, P. Shakkottai, T. S. Luchik, K. M. Aaron, G. Fabris and L. H. Back, Hot wires/films behavior in low temperature gases, *ASME J. Heat Transfer* **114,** 859–865 (1992).
11. K. Harstad, Cryogenic jet mixing model, heat transfer in phase change, *ASME Heat Transfer Division*, Vol. **205,** pp. 79–90 (1992).
12. R. D. McCarty, J. Hord and H. M. Roder, Selected Properties of Hydrogen, NBS Monograph 168, U.S. Government Printing Office, Washington, DC (1981).
13. V. V. Sychev, A. A. Vasserman, A. D. Kozlov, G. A. Spiridonov and V. A. Tsymarny, *Thermodynamic Properties of Nitrogen*. Hemisphere, New York (1987).
14. V. V. Sychev, A. A. Vasserman, A. D. Kozlov, G. A. Spiridonov and V. A. Tsymarny, *Thermodynamic Properties of Oxygen*. Hemisphere, New York (1987).
15. R. B. Scott, *Cryogenic Engineering*. Van Nostrand, Princeton, NJ (1959).